International Journal of
INTELLIGENT SYSTEMS AND APPLICATIONS IN ENGINEERING
ISSN:2147-6799 www.ijisae.org Original Research Paper

Identification of Suitable Telemetry Point Coordinates in Drone Video using Centroid Method for Precise Georeferencing

Vishal Nagpal[1], Dr. Manoj H. Devare[2]

Submitted: 24/04/2023 **Revised**: 27/06/2023 **Accepted**: 06/07/2023

Abstract: Vehicle detection is the most important aspect of traffic monitoring. Unmanned aerial vehicles (UAV) are used to calculate various traffic metrics such as traffic volume and density as well as to handle situations like accidents and traffic congestion in addition to monitoring traffic. The primary objective of this study is to examine the difficulties in accurately georeferencing drone videos to determine the speed of moving vehicles. This study also determined the ideal and minimal number of known telemetry points and their ideal location on video frames (images) in order to ensure accurate telemetry data calculations for all coordinates of the video frame. Since the globe is not flat and because drone payload, camera height, and slant angle might vary, most existing algorithms that use four corner points for georeferencing can be inaccurate. In order to overcome this drawback, the study suggests locating a fifth point coordinate and using it to compute a correction coefficient that can facilitate more precise telemetry point calculations. In addition to experimental data proving the efficiency of the suggested strategy in improving georeferencing accuracy, the study offers a thorough analysis of it. This study found that the centroid method improved data by 1% compared to the four-point approach and the fifth telemetry point in a drone video.

Keywords: *Drone video; Vehicle speed estimation; Georeferencing; Telemetry; Centroid estimation method.*

1. Introduction

In several fields where unmanned aerial vehicles (UAV), such as in infrastructure monitoring and disaster response, are thought to be valuable, rapid and precise direct georeferencing has been gaining relevance. In the past, ground-based unmanned aircraft (UAV) imagery or video streams were either processed further through indirect georeferencing using Ground Control Points (GCP) acquired by geodetic differential Global Navigation Satellite System (GNSS) receivers, or they were broadly referenced through visual analysis within a specific local context. UAVs are being used more frequently every day to monitor traffic. This is due to the fact that UAVs are seen as cost-effective, deliver worldwide data, may be deployed for military and reconnaissance use, are beneficial for agricultural surveys, metrological data collecting, and traffic monitoring, and are deployable for military and reconnaissance use. This creates an interdisciplinary field of study for academic research that is very important in the areas of computer vision, image processing, artificial intelligence, and many others (Elloumi et al., 2019). Optical flow and feature points between frames will estimate each tracked vehicle's speed. Drone altitude, slant range, resolution, and FoV will determine a correction variable. To refine object speeds, this correction variable will be adjusted.

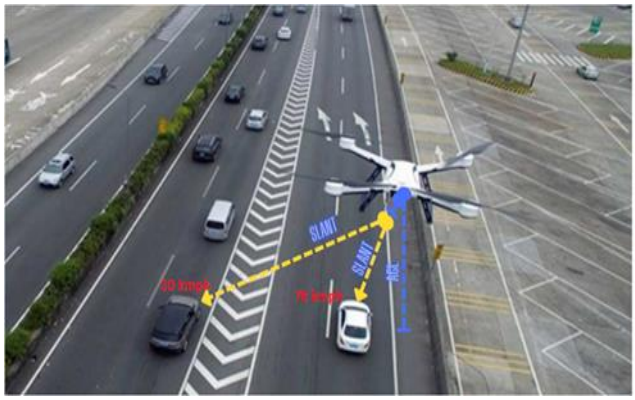

Fig 1: UAV tracking different vehicles covering AGL and Slant Range

[1]*Associate Director, IdeaForge Technology Limited, Navi Mumbai India*
ORCID: 0000-0002-5831-354X
Email: vishal.nagpal@gmail.com
[2]*Professor & HOI AIIT-AUM, Amity University, Navi Mumbai, India*
ORCID: 0000-0002-9530-3914
Email: devare.manoj@gmail.com

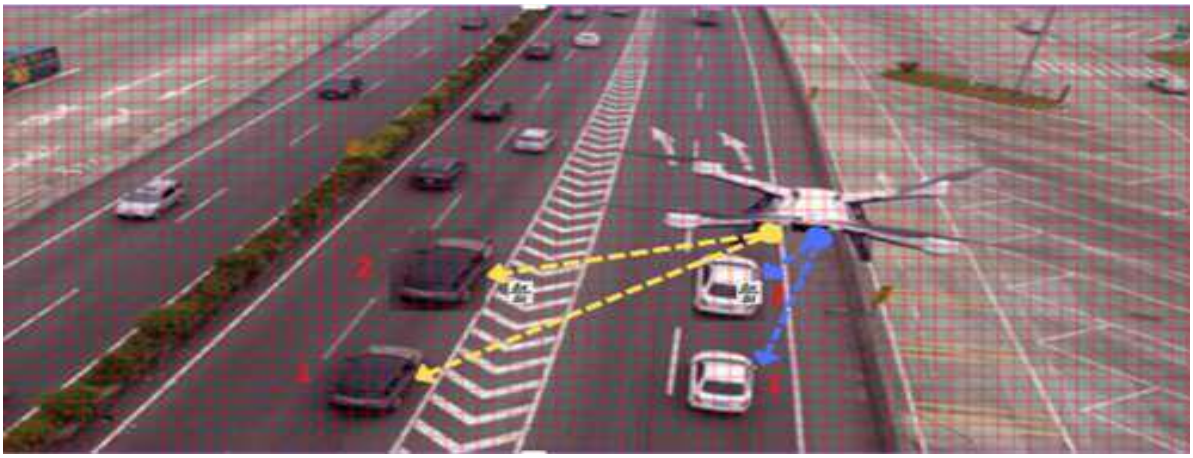

Fig 2: UAV tracking change in pixels based on resolution and estimating pixel velocity

Due to a number of factors, including the non-flat form of the planet, changes in the drone payload and camera height, and variations in slant angle, georeferencing accuracy in drone video frames can be difficult. The position information linked to the four corner points that are frequently utilised for georeferencing may be inaccurate as a result of these circumstances. It may be helpful to find a fifth extra known telemetry point with longitude and latitude data in order to address these issues and boost georeferencing accuracy. The location information collected from the four corner points can then be corrected using this extra point, which can be used to produce a correction coefficient (Haala et al., 2022). The fifth point is incorporated into the georeferencing method in many steps.

This study aims to find the ideal and least number of known telemetry points and their appropriate location on video frames (pictures) to assure correct telemetry data calculations for every video frame location. This publication provides insights for drone video analysis and georeferencing scholars and practitioners. The previous literature relevant to this study is discussed in greater detail in the next section.

2. Literature Review

Geospatial products like DEMs are essential topographic tools for local flood research, according to **Escobar Villanueva et al. (2019).** This study examines how LiDAR elevation data affects DEM creation from fixed-wing UAV images for flood applications. The LiDAR-derived control point (LCP) method in Structure-from-Motion photogrammetry is used to evaluate UAV-derived DEMs. UAV terrain products' flood estimates (volume and area) are compared to LiDAR. LCP-georeferencing is accurate. Semi-automatic terrain data classification makes it suitable for flood investigations. Finally, it shows local LiDAR-UAV photogrammetry complementarity.

Arango et al. (2020) stated that this study developed true reflectance surfaces in the visible portion of the electromagnetic spectrum from small unmanned aerial system (sUAS) photos taken over big bodies of water without ground control points. The research sought to create real reflectance surfaces from which reflectance values may be derived and utilised to determine optical water quality parameters using limited in-situ water quality tests.

According to **Ekaso et al. (2020),** geospatial information from Unmanned Aerial Vehicles (UAV) supports decision-making in many fields, and technical developments drive demand for more complex data products. This study assesses the DJI Matrice 600 Pro's real-time kinematics (RTK) GNSS positioning accuracy.

Bommes et al. (2022) recommended using drone-mounted infrared (IR) cameras and automated video processing algorithms to economically discover aberrant photovoltaic (PV) modules in large-scale PV farms. Traffic monitoring is crucial today, according to **Ali et al. (2022).** Video cameras and induction loops were used for this before. Unmanned aerial vehicles (UAVs) have created new possibilities for this task, and several research initiatives are being done in this area. Aerial photos are difficult to recognise and track due to the high density of objects, difficult view angles, changing illumination, and drone altitudes. This work uses a cascade classifier and centroid tracking to detect and track automobiles.

This prior research suggests identifying a fifth known telemetry point with longitude and latitude information to overcome these problems and increase georeferencing accuracy. This extra point can be used to calculate a correction coefficient for the four corner point position data.

3. Methodology

This study's methodology was the Centroid Method Approach. Ground control points (GCPs) are a very efficient method for georectification. The geometry of the UAS images can be corrected using a mathematical coordinate transformation that is empirically determined using GCPs markers. In 2020, Arango et al. The centroid approach entails locating the centroid of the rectangle

created by the four corners of the frame, which is the intersection of its diagonals. For each new unknown point in the arbitrary coordinate space, a cluster centroid may be determined using the bounding box of these cluster points. While some RTK positioning data techniques offer a planimetric accuracy of direct geo-referencing for the photogrammetric product ranging between 30 and 60 cm, they also significantly increase latency, rendering the basic idea less useful for real-time speed analysis (Ekaso et al., 2020).

The following formula is used to determine the centroid:

Centroid X-coordinate =

$$\frac{(Top-Left\ X-coordinate + Top-Right\ X-coordinate + Bottom-Left\ X-coordinate + Bottom-Right\ X-coordinate)}{4}$$

Centroid Y-coordinate =

$$\frac{(Top-Left\ Y-coordinate + Top-Right\ Y-coordinate + Bottom-Left\ Y-coordinate + Bottom-Right\ Y-coordinate)}{4}$$

The fifth telemetry point's coordinates are calculated after the centroid is calculated using the following formula:

Fifth Point X-coordinate *= Centroid X-coordinate + (Altitude * tan (Slant Angle) * (Top Weight - Bottom Weight))*

*Fifth Point Y-coordinate = Centroid Y-coordinate + (Altitude / cos (Slant Angle) * (Top Weight - Bottom Weight))*

Here, Altitude refers to the drone camera's altitude, Slant Angle to its slant angle, Top Weight to the weight assigned to the frame's top points, and Bottom Weight to the weight assigned to the frame's bottom points. As a GCP, this Centroid point is then used with the Kabsch technique to georeference 3D tiles (Woo et al., 2022). Reducing georeferencing mistakes is made easier by the accuracy of 3D tiles when providing points that correspond to GCPs.

3.1 Calculation – Based Upon Real-Time Data Collected:

Below is a calculation based on real-time data that was gathered for the purpose of this study.

A. INITIAL DATA SET COLLECTED:

The initial data set collected on a random video frame taken from a drone flight:

Table 1: Data set collected

Top-Left Coordinate	(19.1183727813081, 73.0097897714174)
Top-Right Coordinate	(19.1149071495106, 73.0328451600602)
Bottom-Left Coordinate	(19.1130141266718, 73.0115774887186)
Bottom-Right Coordinate	(19.1104512304477, 73.0303793430931)
Assumed Weightage based upon reverse analysis of multiple datasets.	
Bottom points weightage	100% (assumed)
Top point weightage	90% (assumed)
AGL	95m
Slant Range	138m

B. FIFTH COORDINATE CALCULATIONS:

Consider the weight of the bottom points to be 100% since they are closer to the drone camera and have more accurate telemetry data, but the weight of the distant points is 90% on the drone camera and is deemed to be less accurate. It can use the centroid method to determine the coordinates of the fifth telemetry point given the Top-Left, Top-Right, Bottom-Left, and Bottom-Right coordinates of a frame taken by a drone, the weighting of the Top and Bottom

points as 90% and 100% respectively, along with the altitude of 95m and slant range of 138m. First, using the formula below, one can determine the coordinates of the centroid of the four corners.

X coordinate of centroid =

$$\frac{(Top - Left\ X\ +\ Top - Right\ X\ +\ Bottom - Left\ X\ +\ Bottom - Right\ X)}{4}$$

Y coordinate of centroid =

$$\frac{(Top - Left\ Y\ +\ Top - Right\ Y\ +\ Bottom - Left\ Y\ +\ Bottom - Right\ Y)}{4}$$

Substituting the given values:

X coordinate of centroid =

$$\frac{(19.1183727813081\ +\ 19.1149071495106\ +\ 19.1130141266718\ +\ 19.1104512304477)}{4}$$

= 19.11493607

Y coordinate of centroid =

$$\frac{(73.0097897714174\ +\ 73.0328451600602\ +\ 73.0115774887186\ +\ 73.0303793430931)}{4}$$

= 73.02139794

The centroid's altitude offset from the ground can then be calculated as follows:

*Altitude offset = Altitude - (Slant Range * sin (Slant Angle))*

Substituting the given values:

*Altitude offset = 95 - (138 * sin (Slant Angle)) = 95 - (138 * sin^-1(95/138)) = 57.07m*

Finally, it can calculate the coordinates of the fifth telemetry point as follows:

*X coordinate of fifth point = X coordinate of centroid + (Altitude offset * tan (Half Field of View) * (1 - (Top weightage / Bottom weightage)))*

Y coordinate of fifth point = Y coordinate of centroid

Substituting the given values:

*X coordinate of fifth point = 19.11493607 + (57.07 * tan (28.07/2) * (1 - (0.9 / 1))) = 19.11493574 km*

Y coordinate of fifth point = 73.02139794

So, the final coordinates are:

Table 2: Coordinates of the fifth telemetry point using the centroid method

Fifth point Coordinate	19.11493574, 73.02139794
Top-Left Coordinate	19.1183727813081,73.0097897714174
Top-Right Coordinate	19.1149071495106,73.0328451600602
Bottom-Left Coordinate	19.1130141266718,73.0115774887186
Bottom-Right Coordinate	19.1104512304477,73.0303793430931

C. ESTIMATION OF SPEED:

Using the optical flow and feature points between successive frames, the speed of each tracked vehicle will be calculated. Based on the supplied parameters of drone altitude, slant range, resolution, and FoV, a correction variable will be calculated. The calculated speed of each object will be adjusted using this correction variable.

$$Speed = \frac{(X2 - X1)}{t2 - t1}$$

X_2, X_1 - difference of the distance between the frames.

t_2, t_1 – Time Lapse.

4. Results And Discussions

Below is a drone footage frame's border. Hollow circles indicate four known coordinates and a straight line connects them. The centroid position is displayed as a balloon marker in Section B above using these four positions. As seen, the balloon marker is pointed towards the top corners of the supposed rectangular form rather than its centre. By determining the average mean of these five locations, georeferencing any new points is far more accurate.

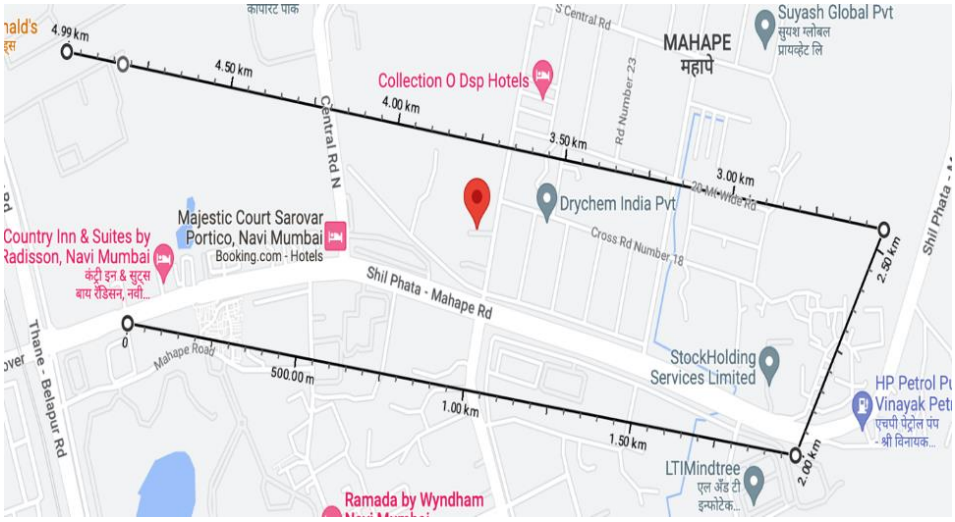

Figure 3: Representation of 5 Coordinates on Map

The table below indicates that the centroid method estimates telemetry data more accurately than the four-point method. Centroid performed 1.0% better than the four-point method. The current method may not work when ground control point determination is problematic. This may change LiDAR-based georeferencing (Escobar Villanueva et al., 2019). The Centroid checkpoint result is better than previous research assessing absolute 3D measurement accuracy using calibrated relative orientation parameters across many cameras.

Table3: Accuracy comparison

Time (s)	Accuracy Comparison with 4 Points Approach			
	GPS Speed (kmph)	***4 Pts. Speed (kmph)***	***5 Pts. Speed (kmph)***	***Accuracy Improvement (In %)***
0:05	45	44.2	44.8	1.3
0:15	48	48.5	47.9	1.2
0:25	50	50.2	50.1	0.2
0:35	46	45.8	46.5	1.5
0:45	49	49.2	48.9	0.6
0:55	47	46.5	46.9	0.9
1:05	51	51.8	50.9	1.7
1:15	48	48.2	47.9	0.6
1:25	44	44.9	44.5	0.9
1:35	47	47.5	47.1	0.9
Average (10 Records)	-	-	-	**1.0**

Figure 4: Comparison of the Accuracy with the 4 points approach

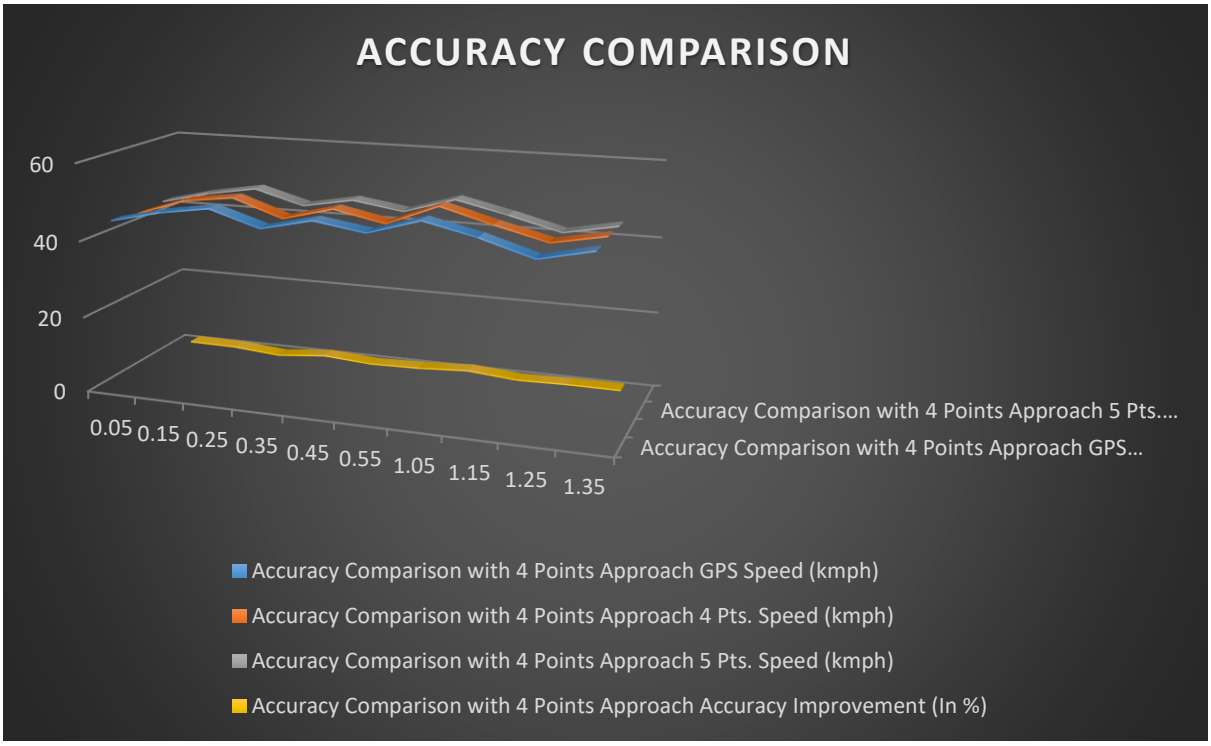

The table above compares the five-point proposed method to four-point speed estimation methods. A GPS sensor measures the speed and "Time (in seconds)" while driving. GPS Speed (kmph) shows the baseline speed of a GPS-equipped car. Column '4 pts Speed (kmph)' calculates speed assuming GPS coordinates of four locations, ideally four corner points, are known and GPS referencing of other points was calculated using the traditional mean average approach. The next column, "5 Pts. Speed (kmph)," covers one more centroid point as part of the research paper's suggested methodology. The final column, "Accuracy Improvement (in%)," details the percentage increase in speed accuracy between 5 points and 4 points in relation to GPS speed. As an example, accuracy improvement is equal to [(5 Pt Speed - 4 Pt Speed)/ GPS Speed * 100]. All of the speeds in this table are expressed in kilogrammes per hour (kmph), and accuracy improvement is rounded to the nearest whole number. The final row of the output displays the mean accuracy improvement (%) for 10 records collected at regular intervals of 10 seconds.

5. Conclusion

In this research, a method using the centroid approach was suggested for calculating the coordinates of the fifth telemetry point in a drone video. The accuracy of this method was also compared to the conventional four-point method in this study, and it was discovered that the centroid method offers a considerable improvement of 1% on the real data obtained, which is quite significant.

References

[1] Huang, H., & Savkin, A. V. (2022). Aerial Surveillance in Cities: When UAVs Take Public Transportation Vehicles. *IEEE Transactions on Automation Science and Engineering*.

[2] Ali, S., & Jalal, A. (2020). Vehicle Detection and Tracking from Aerial Imagery via YOLO and Centroid Tracking.

[3] Elloumi, M., Dhaou, R., Escrig, B., Idoudi, H., Saidane, L. A., & Fer, A. (2019). Traffic Monitoring on City Roads Using UAVs. In *Ad-Hoc, Mobile, and Wireless Networks: 18th International Conference on Ad-Hoc Networks and Wireless, ADHOC-NOW 2019, Luxembourg, Luxembourg, October 1–3, 2019, Proceedings 18* (pp. 588-600). Springer International Publishing.

[4] Haala, N., Kölle, M., Cramer, M., Laupheimer, D., & Zimmermann, F. (2022). Hybrid georeferencing of images and LiDAR data for UAV-based point cloud collection at millimetre accuracy. *ISPRS Open Journal of Photogrammetry and Remote Sensing*, *4*, 100014.

[5] Escobar Villanueva, J. R., Iglesias Martínez, L., & Pérez Montiel, J. I. (2019). DEM generation from fixed-wing UAV imaging and LiDAR-derived ground control points for flood estimations. *Sensors*, *19*(14), 3205.

[6] Arango, J. G., Holzbauer-Schweitzer, B. K., Nairn, R. W., & Knox, R. C. (2020). Generation of geolocated and radiometrically corrected true reflectance surfaces in the visible portion of the electromagnetic spectrum over large bodies of water using images from a

sUAS. *Journal of Unmanned Vehicle Systems*, *8*(3), 172-185.

[7] Ekaso, D., Nex, F., & Kerle, N. (2020). Accuracy assessment of real-time kinematics (RTK) measurements on unmanned aerial vehicles (UAV) for direct geo-referencing. *Geo-spatial information science*, *23*(2), 165-181.

[8] Bommes, L., Buerhop-Lutz, C., Pickel, T., Hauch, J., Brabec, C., & Marius Peters, I. (2022). Georeferencing of photovoltaic modules from aerial infrared videos using structure-from-motion. *Progress in Photovoltaics: Research and Applications*, *30*(9), 1122-1135.

[9] Ali, S., Hanzla, M., & Rafique, A. A. (2022, October). Vehicle Detection and Tracking from UAV Imagery via Cascade Classifier. In *2022 24th International Multitopic Conference (INMIC)* (pp. 1-6). IEEE.

[10] Woo, K., Onsen, A., & Kim, W. (2022). Georeferencing 3D Tiles Generated from Photogrammetry-Derived Mesh Using Ground Control Points. *Journal of Geographic Information System*, *14*(5), 430-443.

[11] Naga Swetha, G. ., & M. Sandi, A. . (2023). A Brand-New, Area - Efficient Architecture for the FFT Algorithm Designed for Implementation of FPGAs. International Journal on Recent and Innovation Trends in Computing and Communication, 11(2), 114–122. https://doi.org/10.17762/ijritcc.v11i2.6135

[12] Ólafur, S., Nieminen, J., Bakker, J., Mayer, M., & Schmid, P. Enhancing Engineering Project Management through Machine Learning Techniques. Kuwait Journal of Machine Learning, 1(1). Retrieved from http://kuwaitjournals.com/index.php/kjml/article/view/112